Updated outline of climate and oceanic conditions to March 2022 for the Indian Ocean, with perspectives on climate change effects on fish catch potential in Maldives and in three coastal upwelling systems

Francis MARSAC[1]
IRD
UMR MARBEC, Seychelles Fishing Authority
Mahé, Seychelles

Abstract

The updated descriptors of ocean status indicate that the Indian Ocean Dipole has been in a neutral phase since 2020, with dominant normal conditions in sea surface temperature. The Dipole is predicted to enter a negative phase in May 2022 until the end of the year, potentially causing thermocline shoaling in the West IO and deepening in the East IO. The thermocline fluctuated in opposite ways between East and West IO. Shallow thermocline conditions took place in the Central IO from March to October 2021, shifting to the West IO in the first quarter of 2022. A strong positive dipole in 2019 boosted (depleted) the plankton production in the East IO (West IO). In 2021, there was higher chlorophyll concentration than normal in the East (+12%) and in the West IO (+8%), and values around the average in the ISSG (+3%) and the Mozambique Channel (-2%). Potential impacts of projected climate change scenarios on fish catch potential over the 21st century are discussed in several regions. In Maldives, the net primary production is projected to decline by ~50% under a high warming scenario (RCP 8.5) and an unsuitable habitat for skipjack tuna to expand over the 21st century. In Oman, the coastal upwelling is projected to intensify, potentially stimulating the biological response at the base of the food web. Conversely, the same simulations foresee a weakening of the Somali upwelling. The South Java upwelling would intensify under the influence of more frequent strong positive Dipole events through the century. There, the response in terms of fish catch potential is subject to debate, either a continuous decline over the century, or an increase to 2025 with a return to current situation in 2050, depending on the structure and the spatial resolution of the ecosystem model used.

1- Data sources

Various sources of data are used in this study:

- Climatic indices. The first category is using sea level pressure data. This includes the Southern Oscillation Index (SOI) that depicts the ENSO cycle, and the Indian Ocean Oscillation Index (IOI, Marsac & Le Blanc, 1998). The second category is based on sea surface temperature-derived, with the Dipole Mode Index (DMI, Saji et al, 1999) reflecting a mode of variability that is specific to the Indian Ocean (and sometimes coupled to the ENSO). The monthly DMI series used here was downloaded from the Hadley Centre, UK (HadISST1.1 product)
- Sea surface chlorophyll-a (SSC) concentration from SeaWifs (1997-2002) and Modis (2003-present) satellite-mounted sensors, giving an index of ocean surface productivity (enhancement or depletion).
- sea surface temperature from the OISSTv2 dataset (*NOAA_OI_SST_V2 data provided by the NOAA/OAR/ESRL PSD, Boulder, Colorado, USA, https://www.esrl.noaa.gov/psd/)* available by month since November 1981 at a spatial resolution of 1°latitude-longitude (Reynolds et al, 2002). Anomalies are based on a 30-year climatology (1981-2010).
- NOAA/NCEP Global Ocean Data Assimilation System (GODAS) providing monthly fields of temperature and other variables for 40 depth levels (5 to 4500 m), along a 1° longitude/0.33°

[1] Email : francis.marsac@ird.fr

latitude grid globally. Here, we use the temperature at depth given by the model to derive the thermocline depth by interpolating the 20°C isothermal depth between consecutive depth levels in the upper 300 m of the water column.

Datasets and methods used to produce the variables are detailed in Marsac (2013). The most recent data incorporated in this analysis are for March 2022.

2- Variability and trends in the oceanic environment

2.1 Climatic indices

The **SOI** indicates that the last El Niño event recorded (negative SOI index) occurred from January to July 2019. Since then, two strong La Niña events occurred, from August to March 2021 and from September 2021 up to present (March 2022). Two mild La Niña events occurred in 2016 and 2017-18. These episodes were separated by 9-12 months long neutral conditions (Fig. 1a).

An ensemble analysis of multiple models predicts a continuation of La Niña regime until the end of 2022: 59% chance during June-August 2022 and 50-55% in the 4th quarter of the year (Fig. 2) (NOAA, 2022). La Niña events cause significant warming of the Western Pacific Ocean, with extension over the maritime continent. Cloudiness and rainfall north of Australia are also enhanced.

The **IOI** was dominated by negative values (reflecting low-pressure anomalies and warm conditions in the West IO) over several years, from 2007 through 2016, followed by alternating conditions with a largely positive IOI in 2016-17, a largely negative IOI in 2019-20 and a moderately positive IOI in 2021 (Fig. 1b). The 2015 and 2020 negative IOI event were synchronous with two El Niño events (negative SOI). The most recent positive IOI events corresponded to La Niña events. Thus, there is some correspondence between IOI and SOI events (Fig. 1b).

The **DMI** has shown mostly positive values since 2006, whereas oscillations between negative and positive episodes occurred in the period 1970-2005 (Fig. 3). The positive DMIs for the past 15 years denote a gradual warming in the West IO. The period 2017 to 2019 was characterized by well-developed positive DMIs. In 2020-21, a return to normal conditions was observed, spanning until the start of 2022 (end of our series). The strongest climatic perturbations occur when positive dipoles arise in coincidence with El Niño, and negative dipoles with La Niña. The positive IOD/El Niño synchrony may cause droughts in the Eastern Indian Ocean (EIO) and severe rainfall anomalies in the Western Indian Ocean (WIO). An opposite response arises when a negative IOD and La Niña are in synchrony.

An ensemble analysis of several models predicts the development of a negative Indian Ocean Dipole from May 2022 through the 4th quarter of 2022 with 85 to 95% probability (Australian Bureau of Meteorology, 2022) (Fig. 4).

All three indices are significantly correlated, with the highest correlation found between IOI and SOI ($rs = +0.47$, $p<.001$). The DMI is more correlated with IOI ($rs = -0.41$, $p<0.001$) than with SOI ($rs = -0.20$, $p<0.001$). The fact that DMI and IOI both depict a mode of variability which is specific to the Indian Ocean can explain such a higher correlation.

We analyzed the SST anomalies in the two area boxes used to compute the DMI: WIO (50°E-70°E / 10°N-10°S) and EIO (90°E-110°S / 0°-10°S) for 2015-2022 (Fig. 5). Firstly, the SST fluctuations in the WIO were essentially with positive anomalies, while the SST fluctuations in the EIO ranged from positive (+1.2°C in January 2016) to negative anomalies (-1.5°C in October 2019). Secondly, the positive temperature anomalies found in both EIO and WIO explain the neutral DMI which has been in place since May 2021.

2.2 Main oceanic features over 2019-2021

Maps of anomalies for SST, the 20°C isothermal depth and SSC are presented in Fig. 6 (a - d).

- The SST signature during the second semester of 2020 showed a gradual return to normal conditions in the equatorial IO (10°N-10°S), after the 2019-2020 positive dipole. A sudden cool anomaly of -0.5 to -1.5°C occurred in January 2021 in the equatorial IO, but this was followed by a return to normal SST conditions in general, with a few patches of low positive SST anomaly (+0.5 to +1°C) distributed in the West, Central and Northeast IO during the 2nd and 3rd quarter

of 2021. The year 2022 started with positive SST anomalies spread throughout the IO basin (with elevated anomaly along 20°S) followed by a return to overall normal conditions in February and March 2022.

- Several patches of shallow thermocline (shoaling of 20 to 50 m) were observed over the second semester of 2020 in the West IO and between latitudes 5°S to 15°S in the Central and East IO. A gradual deepening of the thermocline offshore Sumatra developed from November 2020, culminating in January and February 2021 and vanishing in March 2021. No particular trend was noticed in the thermocline depth, but sustained shallow thermocline was observed in the Central IO, between latitudes 5°S to 20°S, from March to October 2021, extending to the West from November 2021 on, and was still observed in March 2022. Anomalously deep thermocline (deepening of 20 to 60 m, depending on the months) was observed in the extreme north Arabian Sea throughout the time series analysed.

- During the southwest monsoon of 2020 and 2021, the cloud cover in the Arabian Sea was quite dense preventing any sea colour measurements by satellite sensors. Two patches of elevated SSC (> 0.4 mg m^{-3}) developed in the West IO and at the southern tip of Indian and Sri Lanka in July and August 2020. The western patch vanished in September, and was replaced by a negative SSC anomaly off Somalia until December 2020. The patch south of India exhibited highly positive SSC until November 2020. During the same time, depleted SSC conditions were observed off Sumatra and South Java, in the East IO. During the first quarter of 2021, SSC anomalies were only found in the West IO, with largely enhanced SSC along the coasts of Yemen and Oman, whereas SSC negative anomalies took place in the central Arabian Sea. Patches of positive SSC anomalies were noticed in the West IO until March 2020, then vanished to return to overall normal conditions until June 2021. The southwest monsoon 2021 showed mostly depleted SSC in the Somali upwelling and elevated SSC anomalies south of India and Sri Lanka. SSC remained high in the north-central IO throughout the end of 2021 whilst areas of low SSC were observed in the central Arabian Sea. Large monthly variability in SSC occurred during the 1st quarter of 2022, with overall depleted conditions in the Arabian Sea except a large area of elevated chlorophyll (> 0.4 mg m^{-3}) in February 2022. Normal SSC conditions were observed in March 2022 in the rest of the Indian Ocean.

3- Inter-annual variability and primary productivity trends in four ecoregions of the Indian Ocean

The same four large ecoregions that were initially presented by Marsac & Demarcq (2019) were used here. We consider two ecoregions (MONW in the West, MONE in the East, separated at 77°E) within the large MONS Longhurst province (Longhurst, 1998). Our MONW ecoregion also encompasses the Somalian part of the Longhurst's ARAB province. We also delineate an ecoregion for the Mozambique Channel (MOZ) corresponding to the northern region of the Longhurst's EAFR province but excluding the east coast of Madagascar. Finally the 4th ecoregion matches the almost entire Longhurst's ISSG province. The four ecoregions (Fig. 7) are assigned in the following boundaries:

- MONW : 40°E - 77°E / 10°N – 12°S
- MONE : 77°E - 120°E / 10°N – 12°S (excluding regions extending east of Sumatra and north of Java)
- MOZ : 30°E – 47°E / 12°S – 30°S
- ISSG : 47°E – 120°E / 12°S – 30°S

In order to compare the overall productivity of each ecoregion, we computed the SSC annual average as displayed in Fig. 8. The MOZ region is the most productive one, MONW ranks second, MONE ranks third and the less productive region is the ISSG.

MOZ SSC concentration (annual average) ranged from 0.35 to 0.43 mg.m^{-3} with two periods of higher productivity: 1998 to 2002 (mean=0.42 mg.m^{-3}), 2015-2020 (mean=0.41 mg.m^{-3}) separated by 12 years or relatively lower productivity. The lowest SSC value was observed in 1997 when a strong El Niño and positive dipole was developing. The mesoscale vertical dynamics caused by eddies propagating through the Mozambique Channel and the chlorophyll-rich waters of the Mozambican and western Madagascan

shelfs, transported offshore by the action of eddies, contribute to generate an average enhanced productivity in this region.

MONW and MONE SSC concentration showed the same trend between 2015 and 2018 with enhanced conditions, the chlorophyll being slightly more elevated (+0.03 mg m^{-3}) in the East compared to the West IO. The chlorophyll varied in opposite way in 2019 under the influence of the positive dipole depleting chlorophyll in the West and enhancing chlorophyll in the East IO.

Finally, SSC in ISSG fluctuated within a short range, between 0.09 and 0.13 $mg.m^{-3}$ denoting oligotrophic conditions. Slightly higher concentration was observed through 1999-2001 and during the last 5 years of the series.

The series were normalized to perform a direct comparison of inter-annual changes across ecoregions. The normalization consists in calculating the deviation (in %) of each year to the pluri-annual mean, in each region. The normalized time series (Fig. 9) exhibit several features already discussed in Marsac (2021). The most recent prominent anomaly is caused by the 2019 positive Indian Ocean dipole, with 33% more chlorophyll above normal in the East IO and 11% less chlorophyll than normal in the West IO. The updated annual value for 2021 indicates higher phytoplankton biomass than normal in the East (+12%) and in the West IO (+8%), and around the average in the ISSG (+3%) and the Mozambique Channel (-2%).

4- Sub-regional trends in surface chlorophyll

In this section, we investigate SSC trends in the Maldives region, and in three upwelling systems from July 2002 to March 2022: Somali and Oman upwelling in the West IO, and the South Java upwelling in the East IO (Fig. 10).

Maldives

The SSC annual cycle in Maldives, as averaged in our spatial grid of 1°longitude x 0.33° latitude, does not exhibit a wide amplitude (from 0.12 mg m^{-3} in April to 0.22 mg m^{-3} in January). Annual averages were calculated, then deviations in % to the 2002-2021 mean (Fig 11). The fitted spline to the annual values ($p<0.05$) shows clearly an oscillation between episodes of above-normal chlorophyll productivity (1998 to 2005, 2016 to 2021) and a long episode of depleted SSC conditions, from 2006 to 2015. The last two years of the series (2020, 2021) indicate a gradual return to normal conditions. The perspective for the 21st century, under a high warming scenario (RCP 8.5), is a significant decline (-50%) of the net primary production in the Maldives by 2100. Such conditions would lead to a spatial expansion of the unsuitable habitat for skipjack tuna near and over the Maldives EEZ to be seen from 2040 onwards (Dueri et al, 2014).

Oman upwelling

The chlorophyll annual cycle is very well marked off Oman, with two productive seasons in January-March and July-September. The winter bloom (Jan-Mar) is caused by the nutrient enrichment of the surface layer resulting from wintertime convective mixing in the Arabian Sea. This primary production is transported long the coast by the Oman Coastal Current (OCC) flowing to the Southwest during that monsoon phase (Wiggert et al, 2005). The cloud cover is minimal in the absence of atmospheric convention and satellite measurements are informative. The second bloom occurs during the summer monsoon (Jun to Sep), as a result of a coastal upwelling driven by the OCC which reverses and flows to the Northeast during that phase of the monsoon cycle. The cloud cover is maximal and satellite measurements are scarce during the summer monsoon. Therefore ocean colour satellite measurements cannot be compared between seasons. Consequently, we computed an annual average of monthly SSC and the corresponding deviations to the mean 2002-2021, considering only pixels with less than 40% of cloud cover. The deviation in % to the 2002-2021 mean was calculated and shown in Fig 12a. The series exhibits 4 years with positive deviations above 10% (11 to 21%) in 2003, 2006, 2012 and 2019. Conversely, there were 3 years with negative deviations larger than 10% (-11% to -19%). The series does not indicate any particular trend (a spline fit turned out non-significant), rather annual fluctuations between lesser and higher productive conditions. The final years of the series (2020 and 2021) display normal conditions. In the likely hypothesis that tuna production is partly driven by the ocean

productivity, the data shown in this series cannot explain the 4-fold increase of tuna catches by Oman between 2015 and 2020. Reasons have to be found elsewhere. For 21st century projections, we refer to simulations carried out by a high resolution ocean model (ROMS) where an historical hindcast and a forecast based on IPCC scenarios (RCP 8.5) were compared (Praveen et al, 2016). These authors predict an intensification of the upwelling along the coast of Oman in a warming scenario over the 21st century, hence increasing the productivity in these waters from June to September. Such a forecast would lead to enhancement in the food chain leading to tunas and other top predators.

Somali upwelling

The chlorophyll annual cycle in the Somali region is tuned to the reversal of the monsoon, then showing two seasonal peaks. Relatively elevated phytoplankton biomass (0.4 mg m^{-3} over the study area) takes place in winter, from December to March, when the productive waters from the Arabian Sea are transported along the Somali coast by the Somali coastal current flowing south-westward during that phase of the monsoon cycle. The second season is the productive upwelling that develops from June to September, with concentrations ranging from 0.7 to 1 mg m^{-3}. The cloud cover is low then it is possible to evaluate the chlorophyll deviations to the 2002-2021 mean for each season (Fig. 12b). In general, the deviations for both seasons fluctuate in coherence. Splines fitted to each series ($p < 0.05$) depict similar interannual fluctuations across seasons: a regime of elevated SSC during 2002-2005 and 2017-2018, and a regime of depleted SSC during 2006-2016 and 2019-2021. These regimes indicate fluctuations in the upwelling intensity over the study period. On the longer term, the simulations based on RCP 8.5 (mentioned earlier for the Oman upwelling) predict a weakening of the Somali upwelling in a warming scenario, that is opposite to the trend foreseen for the Oman upwelling (Praveen et al, 2016).

South Java upwelling

The chlorophyll cycle in South Java waters exhibits a single productive season from July to October, associated to a wind-induced Ekman divergence producing a coastal upwelling. No particular trend is noticed over the study period (a spline fit turned out non-significant). The largely positive SSC deviations (> +60%) occurred during the development phase of positive Indian Ocean dipoles and Niño events in 2006 and 2019 (Fig 12c). During these events, the deviations were largely negative in the West IO. In 2020-21, the ocean productivity was slightly below normal off South Java. A lower phytoplankton biomass corresponds generally to La Niña events (2005, 2010) combined to warm events in the East IO (e.g. 2016). For the 21st century, Cai et al (2014) project that the frequency of extreme positive dipoles will increase by a factor of almost 3 in a high warming scenario (RCP 8.5), with a large potential to increase the productivity in the West and South Indonesian waters. A recent study using the Pauly and Christensen (1995) model, based on a 10% transfer efficiency between trophic levels and a ratio of fish biomass to carbon weight of 9:1, predicts a slight increase in small pelagic fish biomass (trophic level around 3) by 2025 in the South Indonesian waters, followed by a return to the current status by 2050, in a moderate warming scenario (RCP 4.5) (Koropitan et al, 2021). A different outcome is projected by another study using more complex ecosystem models (Cheung et al, 2018), that predict a ~20% and ~-60% reduction of catch potential, respectively in 2050 and 2100, under a high warming scenario (RCP 8.5). Such catch potential mostly concerns small pelagic fish in the south Indonesian waters, but as they contribute to the tuna diet, they have implications on local tuna abundance.

5- Summary

The Indian Ocean Dipole has been in a neutral phase since 2020, with dominant normal conditions in sea surface temperature although few transient warm or cold anomalies were observed during that phase. The DMI is predicted to enter a negative phase in May 2022 until the end of the year, which could trigger thermocline shoaling in the WIO and deepening in the East IO. The thermocline fluctuated in opposite ways between East and West IO, but a shallow thermocline has been dominating in the Central IO from March to October 2021, and shifted to the West IO during the first quarter of 2022. Chlorophyll concentration has been fluctuating regionally between depleted and enhanced conditions in 2020 through 2022, with an extremely high phytoplankton biomass measured in the North IO in February 2022. Considering large ecoregions, the 2019 strong positive dipole boosted (depleted) the plankton production in the East IO (West IO). In 2021, there was higher phytoplankton biomass than normal in

the East (+12%) and in the West IO (+8%), and biomass around the average in the ISSG (+3%) and the Mozambique Channel (-2%).

Perspectives are drawn for the 21st century by model simulations based on climate change scenarios. In the Maldives, the ocean productivity is predicted to decline throughout the century with potential negative impacts on foraging conditions for tunas, in addition to elevated sea temperature that will lead to the development of unsuitable habitat for skipjack tuna. In Oman, since 2016, chlorophyll concentrations remained close to the average (except in 2019, with a >10% positive anomaly) and we cannot detect any increase in ocean productivity in the upwelling. During that period, catches by Oman were multiplied by 4, and such an increase cannot be related to any positive change in the biotic carrying capacity from an ocean colour perspective. The intensity of the coastal upwelling in Oman is predicted to increase during the century, and this could provide favourable foraging conditions for small and large pelagic tunas. The prospect for the Somali upwelling is opposite to the Oman upwelling. Eventually, the South Java upwelling is projected to increase along with an intensification and higher frequency of positive Indian Ocean dipoles, but the inference to fish catch potential is subject to debate, as the link is mediated by complex processes not well captured when underlying physical models use too coarse resolution (100-200 km).

Acknowledgements

We are grateful to the Climate Centre of the Seychelles Meteorological Authority, and particularly to Beryl Andrade, a quality control technician of this Centre, for the provision of sea level pressure data used to compute the IOI. We also acknowledge Dr Hervé Demarcq, IRD, for providing the updated chlorophyll L4 dataset of Modis.

References

Bureau of Meteorology, Australia (2022). Indian Ocean Dipole outlooks. http://www.bom.gov.au/climate/enso/#tabs=Indian-Ocean

Cai, W., Borlace, S., Lengaigne, M., van Rensch, P., et al. (2014a) Increasing frequency of extreme El Niño events due to greenhouse warming. *Nature Climate Change*, 4, 111–116.

Cheung, W.W.L., Bruggeman, J., & Butenschön, M. (2018). Projected changes in global and national potential marine fisheries catch under climate change scenarios in the twenty-first century. *In* M. Barange, T. Bahri, M.C.M. Beveridge, K.L. Cochrane, S. Funge-Smith (Eds) Impacts of climate change on fisheries and aquaculture: synthesis of current knowledge, adaptation and mitigation options (Chapter 4), *FAO Fish Aquac Tech Paper* 627, pp 63-85.

Dueri, S., Bopp, M. & Maury, O. (2014) Projecting the impacts of climate change on skipjack tuna abundance and spatial distribution. *Global Change Biology*, 20, 742–753.

Koropitan, A.F., Nabil, Osawa, T. (2021). Modelling small-pelagic fish biomass on the Indonesian seas: climate variability and climate change impacts. *IOP Conf. Series: Earth and Environmental Science,* 944, 012069 doi:10.1088/1755-1315/944/1/012069

Longhurst, A. (1998). The ecological geography of the sea. Academic Press.

Marsac, F. (2013). Outline of climate and oceanographic conditions in the Indian Ocean: an update to August 2013. *15th Session of the Working Party on Tropical Tuna*. IOTC-2013-WPTT15-09, 14 p.

Marsac, F. (2021). Outline of climate and oceanographic conditions in the Indian Ocean: an update to mid-2021. *23rd Session of the Working Party on Tropical Tuna*. IOTC-2021-WPTT23-14, 16 p.

Marsac, F., Demarcq, H. (2019). Outline of climate and oceanic conditions in the Indian Ocean: an update to *mid*-2019. *21st Session of the Working Party on Tropical Tuna.* IOTC–2019–WPTT21–24, 19 p.

Marsac, F., Le Blanc, J-L. (1998). Interannual and ENSO-associated variability of the coupled ocean-atmosphere system with possible impacts on the yellowfin tuna fisheries of the Indian and Atlantic oceans. In: J.S. Beckett (Ed). *ICCAT Tuna Symposium. Coll. Vol. Sci. Pap*., L(1) : 345-377.

NOAA, 2022. Climate Diagnostics Bulletin March 2022. Near real-time ocean/atmosphere, monitoring, assessment and prediction.

Pauly, D., Christensen, V. (1995). Primary production required to sustain global fisheries. *Nature* 374 255-257.

Praveen, V., Ajayamohan, R.S.), Valsala, V., Sandeep, S. (2016) Intensification of upwelling along Oman coast in a warming scenario. *Geophys. Res. Lett*. 10.1002/2016GL069638.

Reynolds, R.W., Rayner, N.A., Smith, T.M., Stokes, D.C., and Wang, W. (2002): An improved in situ and satellite SST analysis for climate. *J. Climate*, 15, 1609-1625

Saji, N.H., Goswani, B.N., Vinayachandran, P.N., Yamagata, T. (1999). A dipole mode in the tropical Indian Ocean. *Nature* 401: 360-363

Wiggert, J.D., Hood, R.R., Banse, K., Kindle, J.C. (2005). Monsoon-driven biogeochemical processes in the Arabian Sea. *Prog Oceanogr*, 65, 176-213.

(a)

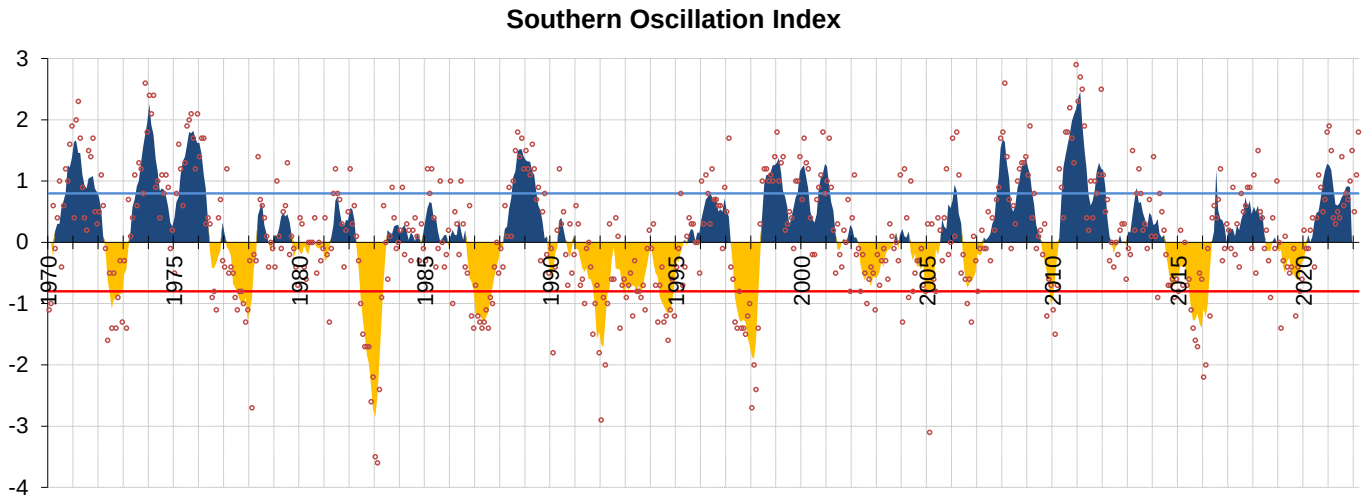

(b)

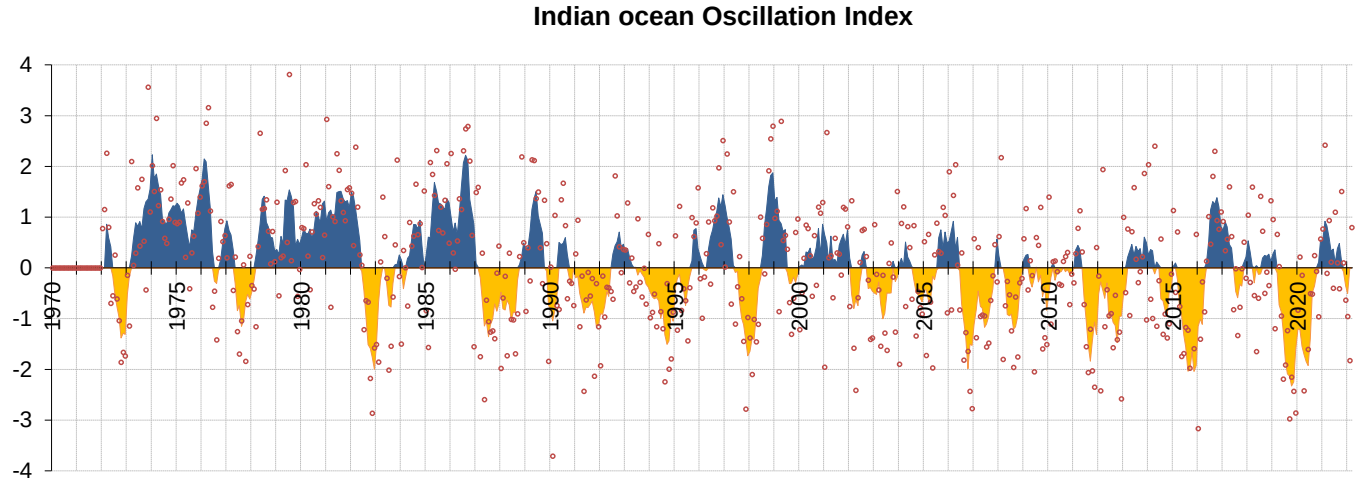

Fig.1 – (a) The Southern Oscillation Index (SOI) and (b) the Indian Oscillation Index (IOI), January 1970 to March 2022. The color shaded area represents the 5-month moving average, whereas observed monthly values are shown in red dots. In the upper panel, El Niño events correspond to the extreme negative values (below the red threshold line) whereas La Niña events are described by the extreme positive values of the SOI (above the blue threshold line).

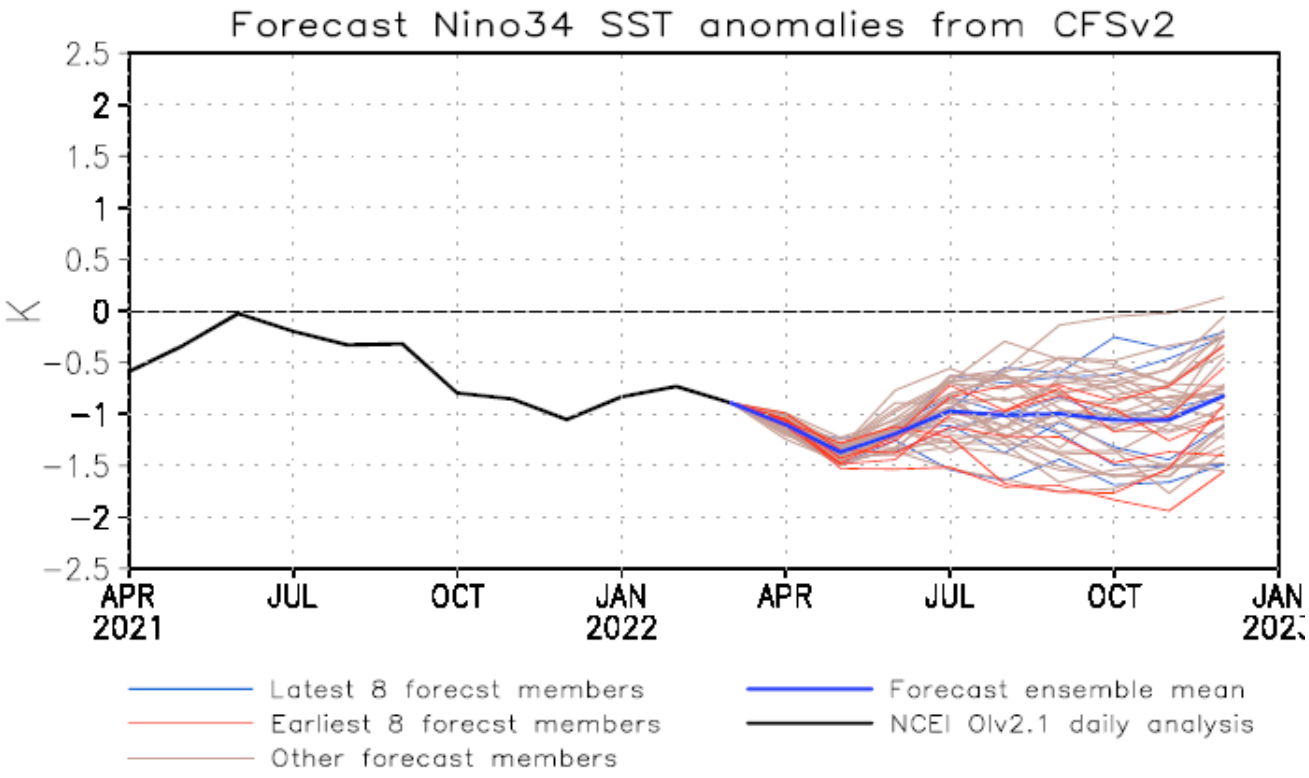

Fig.2 – SST anomalies forecast for Niño 3-4 region (East Pacific ocean) indicating the forecasted trend of the SOI from March to December 2022 (NOAA, 2022)

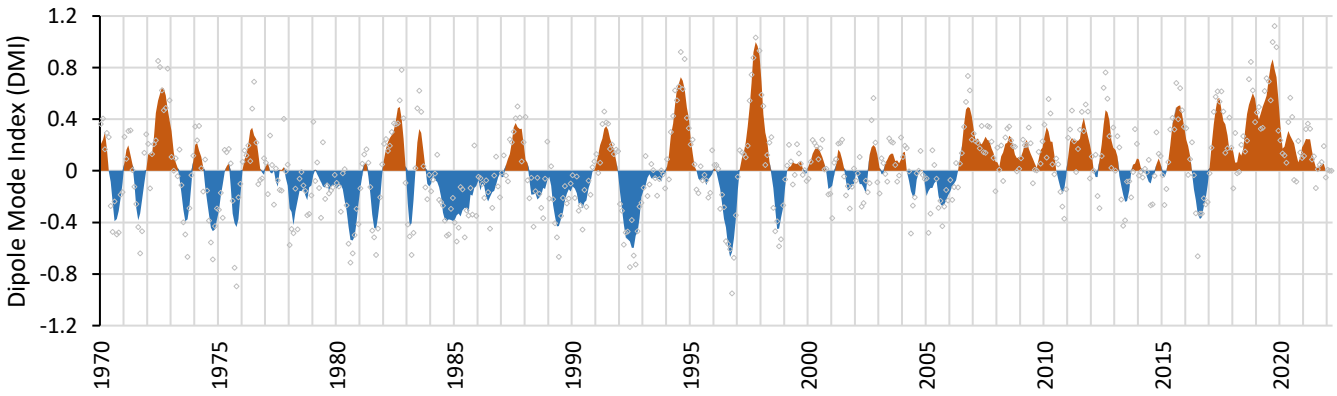

Fig.3 - Dipole mode (DMI), January 1970 – January 2022. The shaded area of DMI is a 5-months moving average whereas observed monthly values are represented in grey empty dots. For a given anomaly, IOI and DMI are frequently in opposite sign. Source: Hadley Centre, UK (HadISST1.1 product).

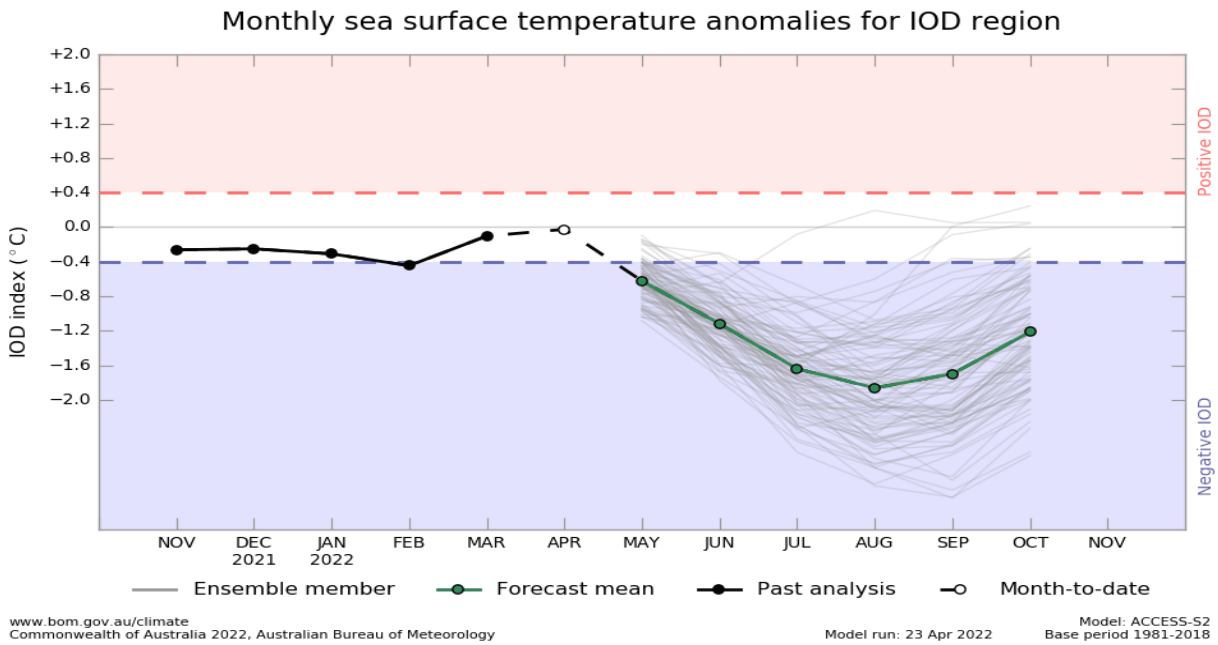

Fig.4 – Dipole mode forecast through predicted monthly sea surface anomalies for the Dipole mode region (Australian Bureau of Meteorology (*http://www.bom.gov.au/climate/enso/#tabs=Indian-Ocean*). Observations span until April 2022, and predictions are from May to October 2022.

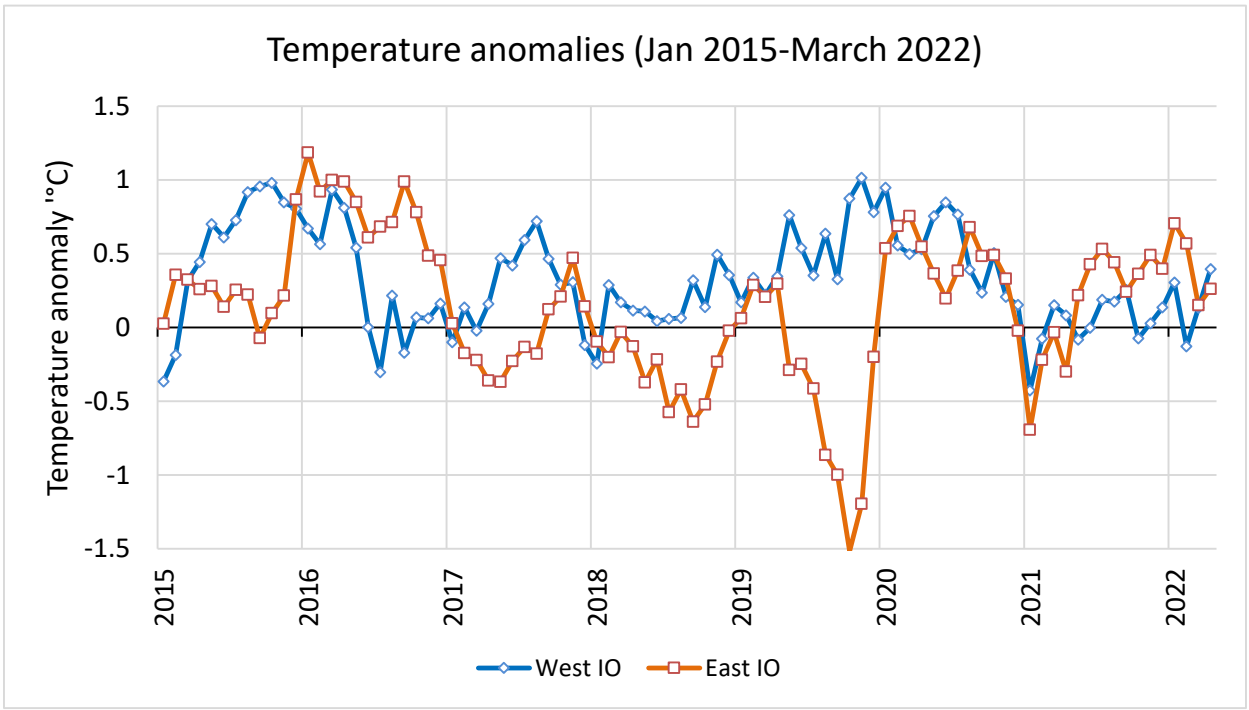

Fig.5 -Monthly SST anomalies in the Western and Eastern area boxes used to compute the DMI, for January 2015 to March 2022. WIO box: 50°E-70°E / 10°N-10°S , EIO box: 90°E-110°E / 0°-10°S (source: OISSTv2)

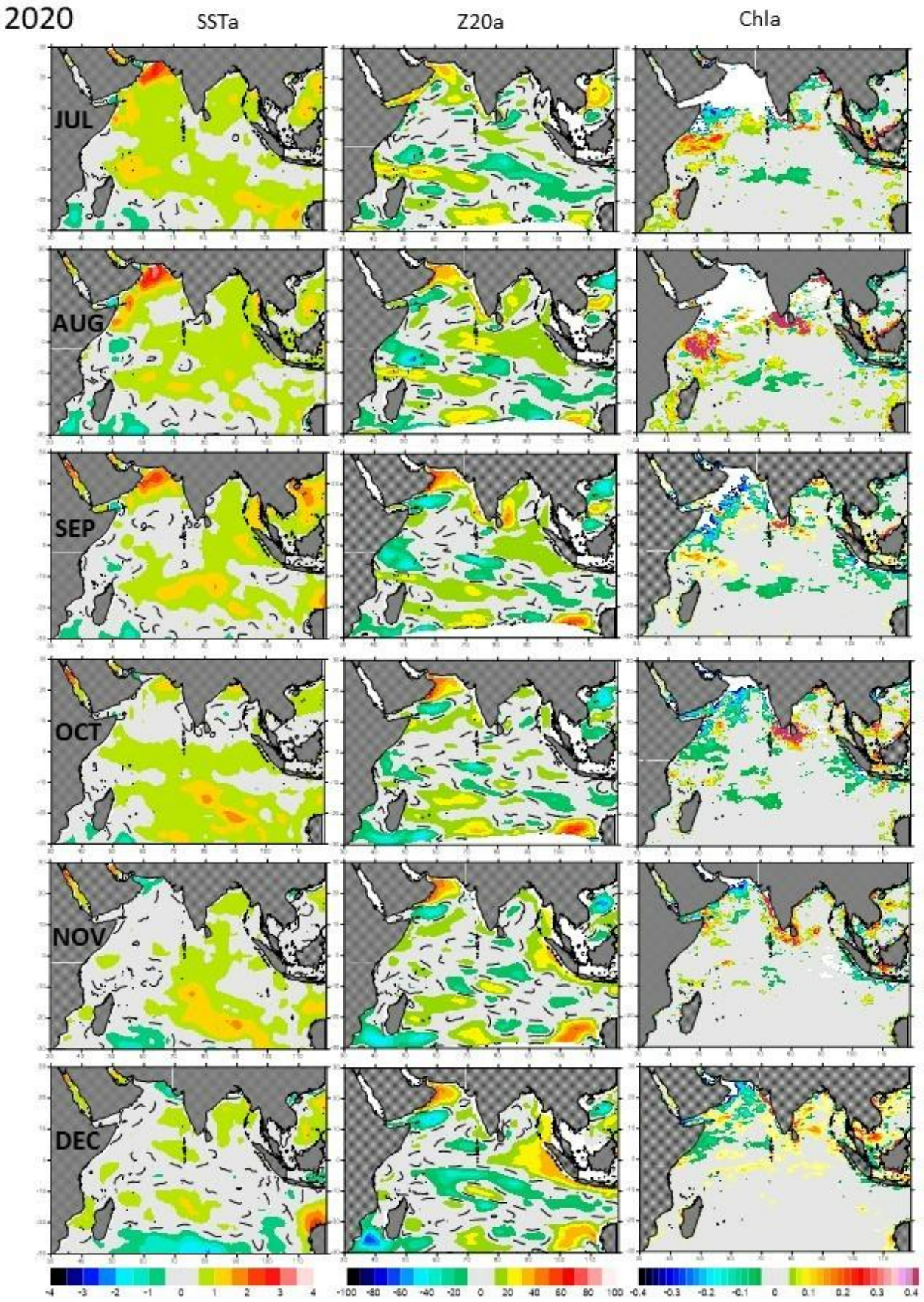

Fig. 6a – Geographic distribution of anomalies for sea surface temperature (°C, left), 20°C isothermal depth (m, middle) and sea surface chlorophyll (mg.m^{-3}, right) for the second semester of 2020. Grey shading indicates minor anomalies (noise) about the mean. Thus, only the more significant anomalies (colour shading) are highlighted.

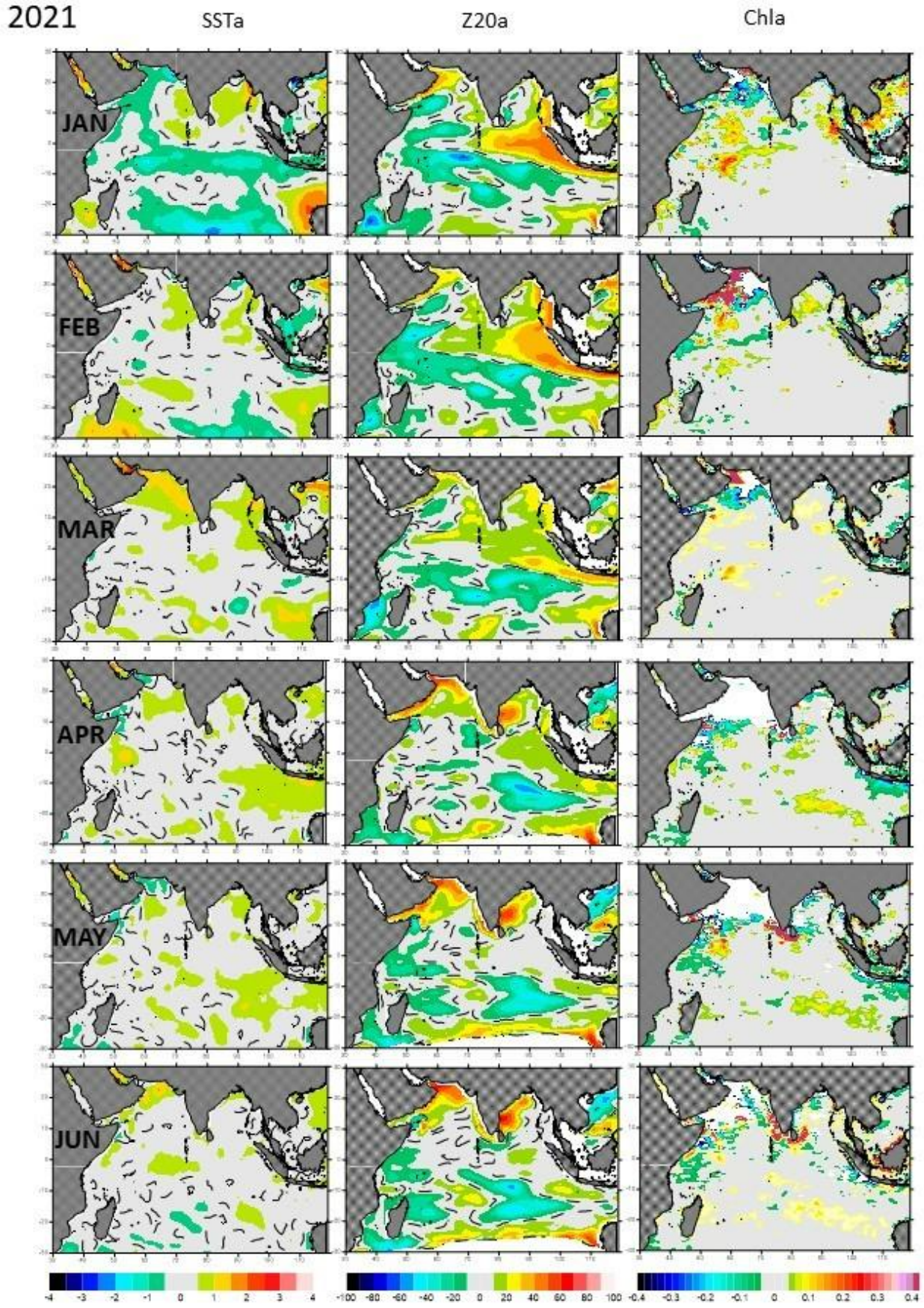

Fig. 6b– Same as above, for the first semester of 2021.

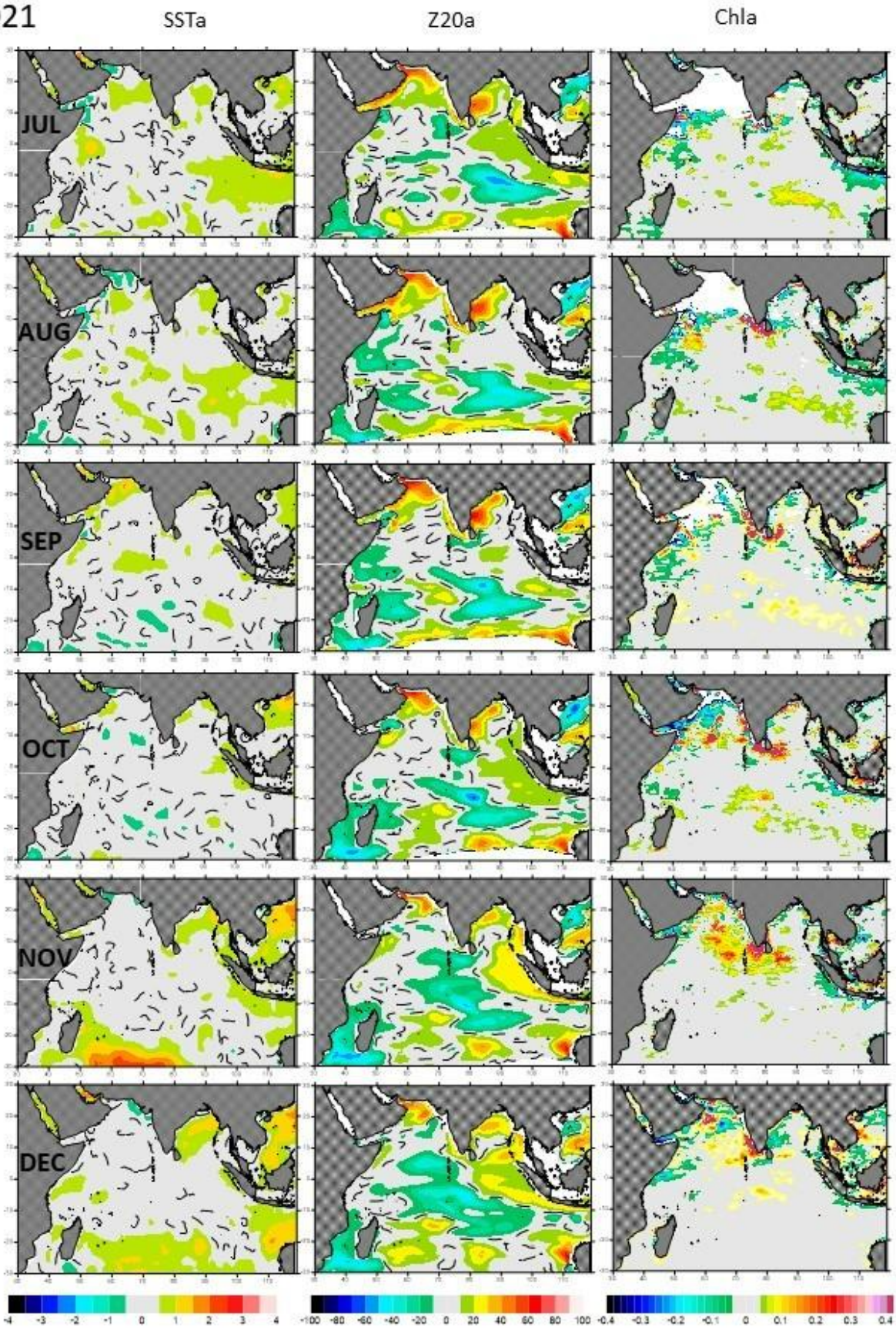

Fig. 6c – Same as above, for the second semester of 2021.

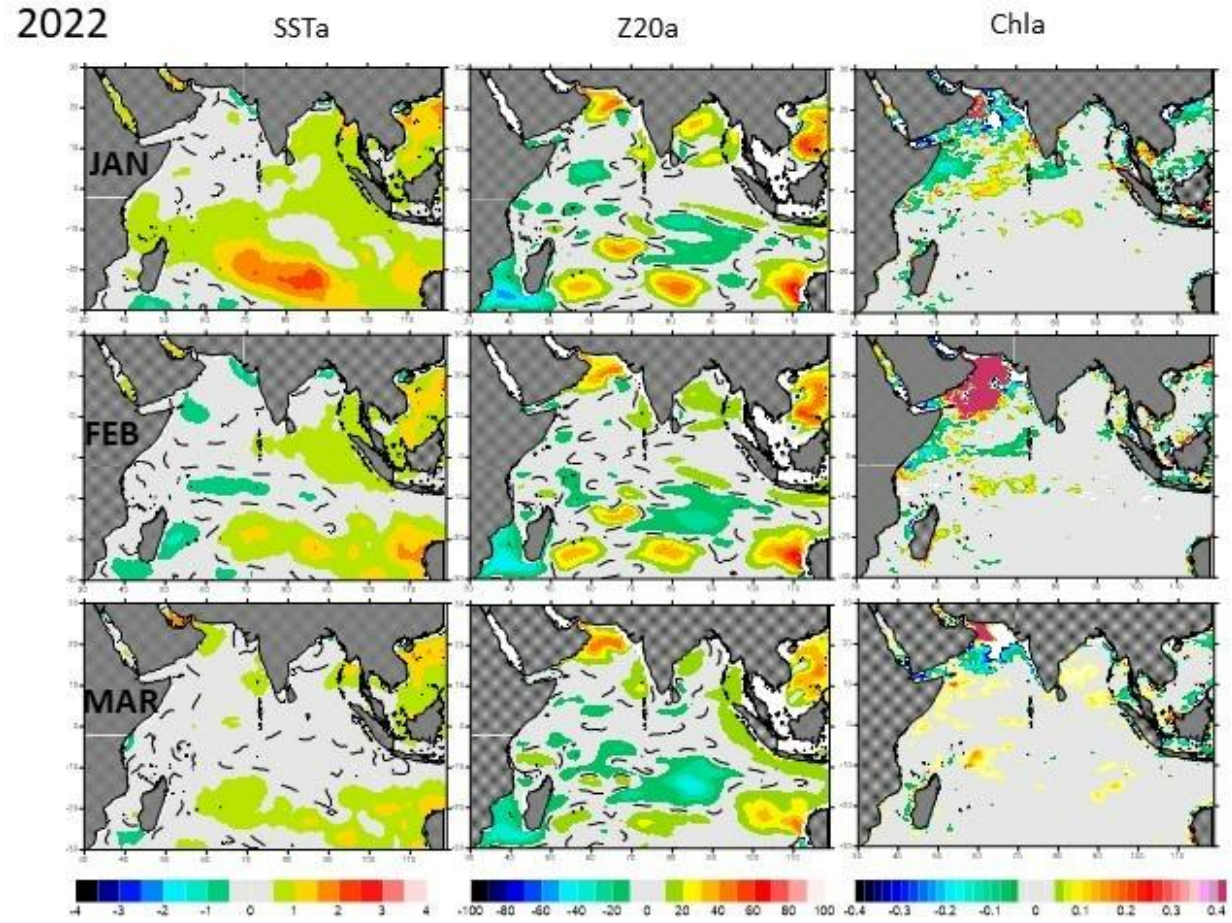

Fig. 6d – Same as above, for the first quarter of 2022.

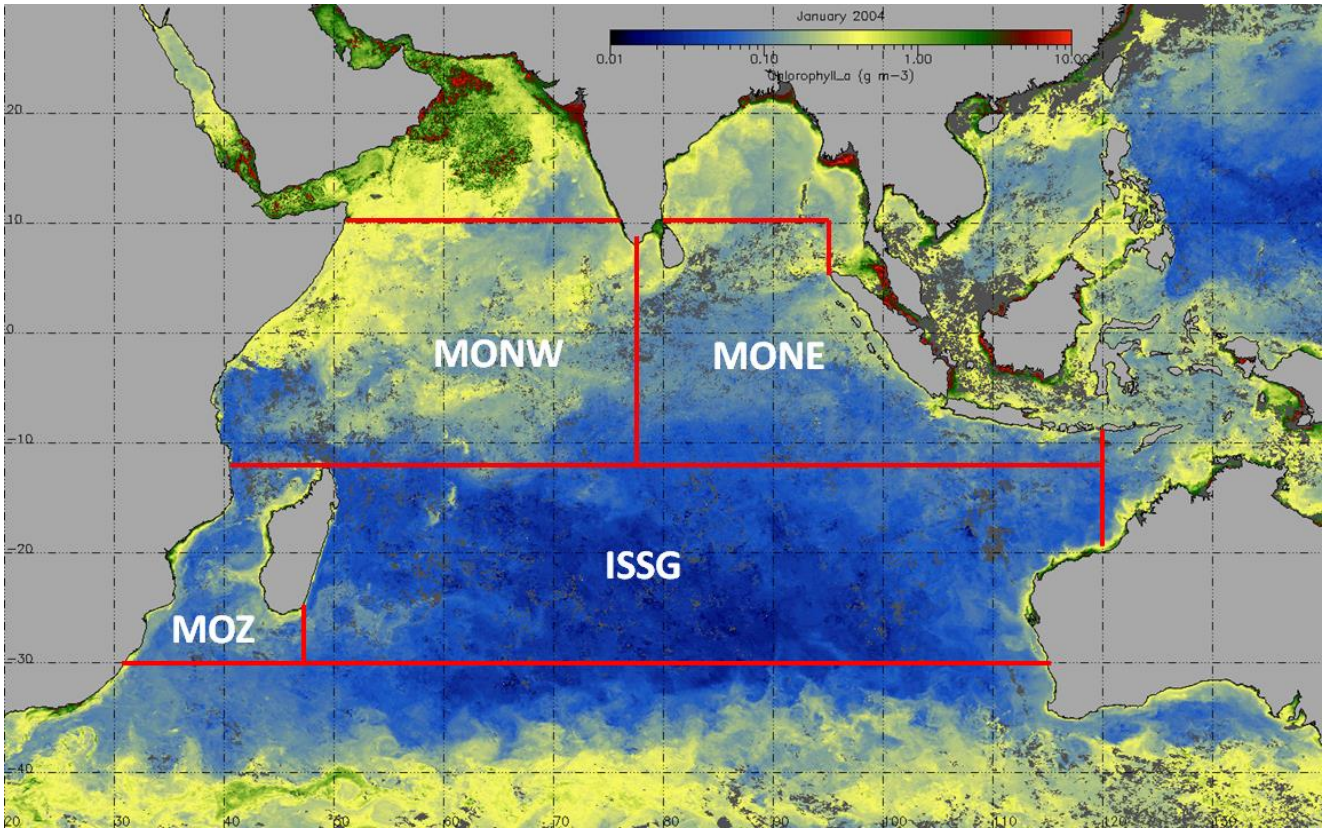

Fig. 7 – Boundaries of the four ecoregions used in this paper. The background image is the chlorophyll concentration measured by MODIS in January 2004.

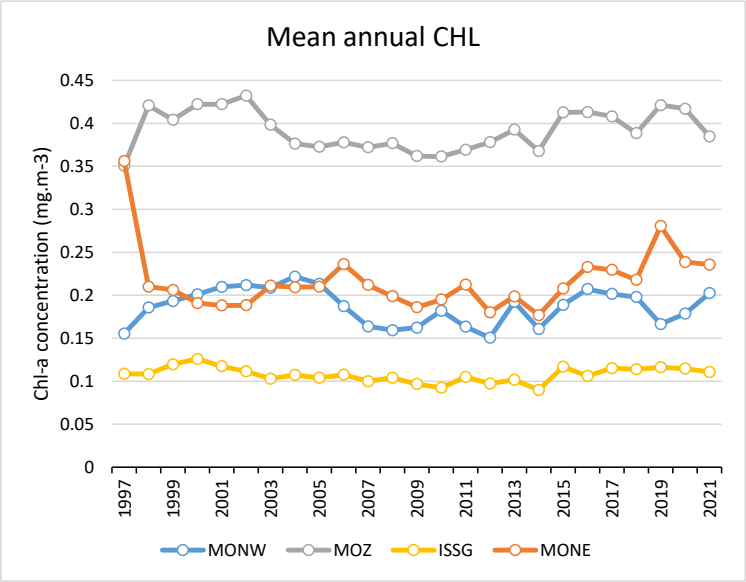

Fig. 8 - Mean annual SSC for each large ecoregion, Sep 1997 to Dec 2021

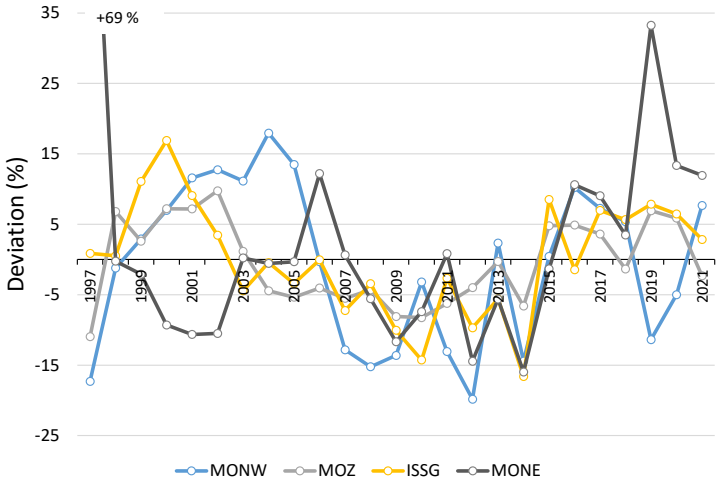

Fig. 9 – Deviation (in %) to the mean multi-annual SSC by large ecoregion, Sept 1997 to Dec 2021

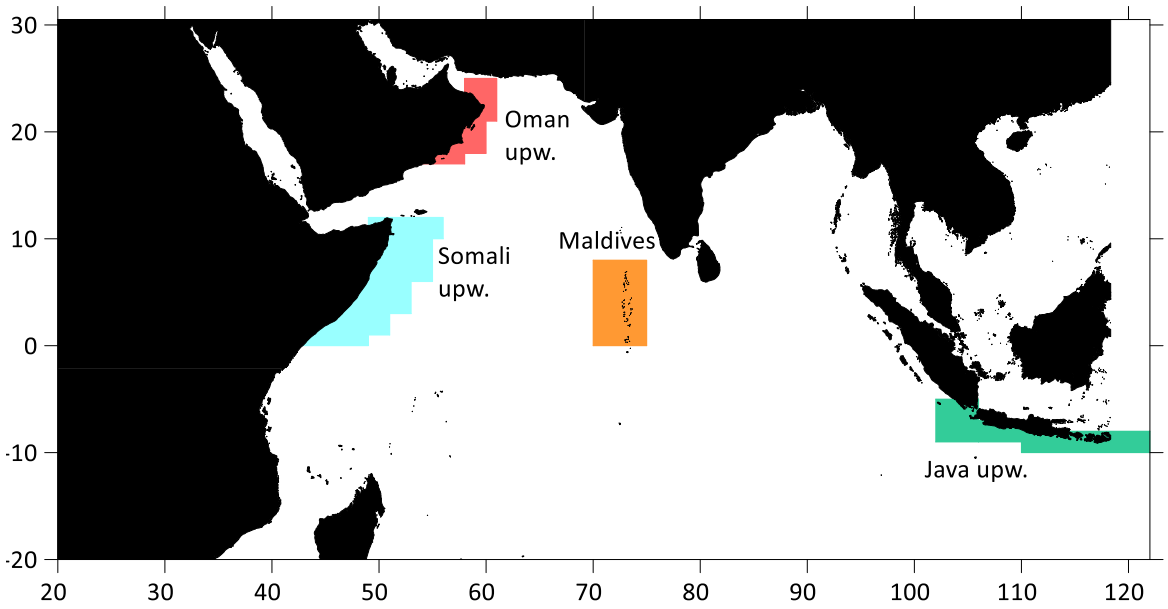

Fig. 10 – Delineation of the three upwelling systems and the Maldives region where chlorophyll trends are calculated

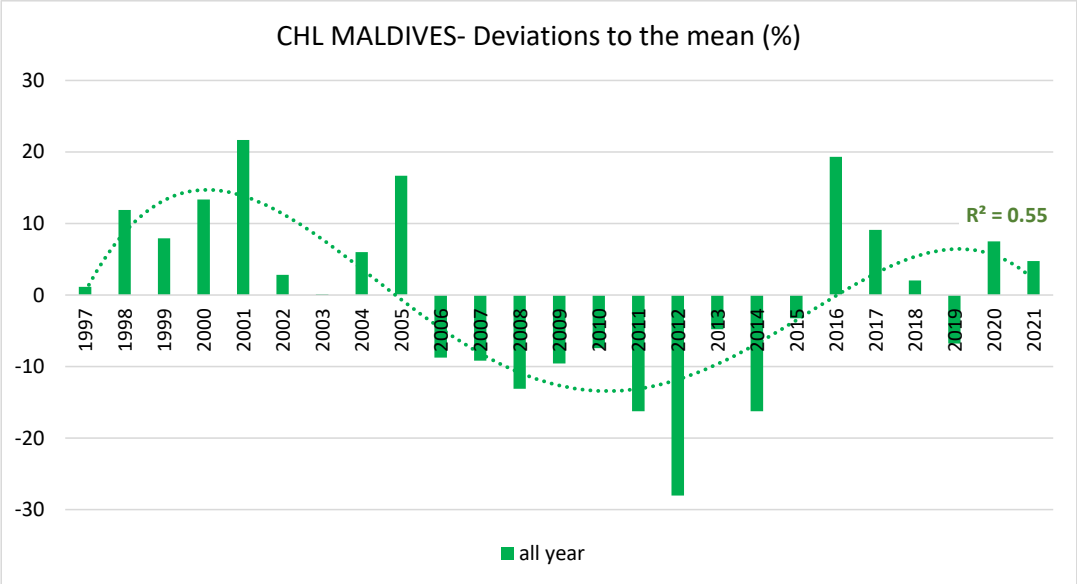

Fig. 11 – Chlorophyll concentration (standardized as deviation in % to the mean) in Maldives (70°E-75°S / 0°-8°N), for 2002-2021.

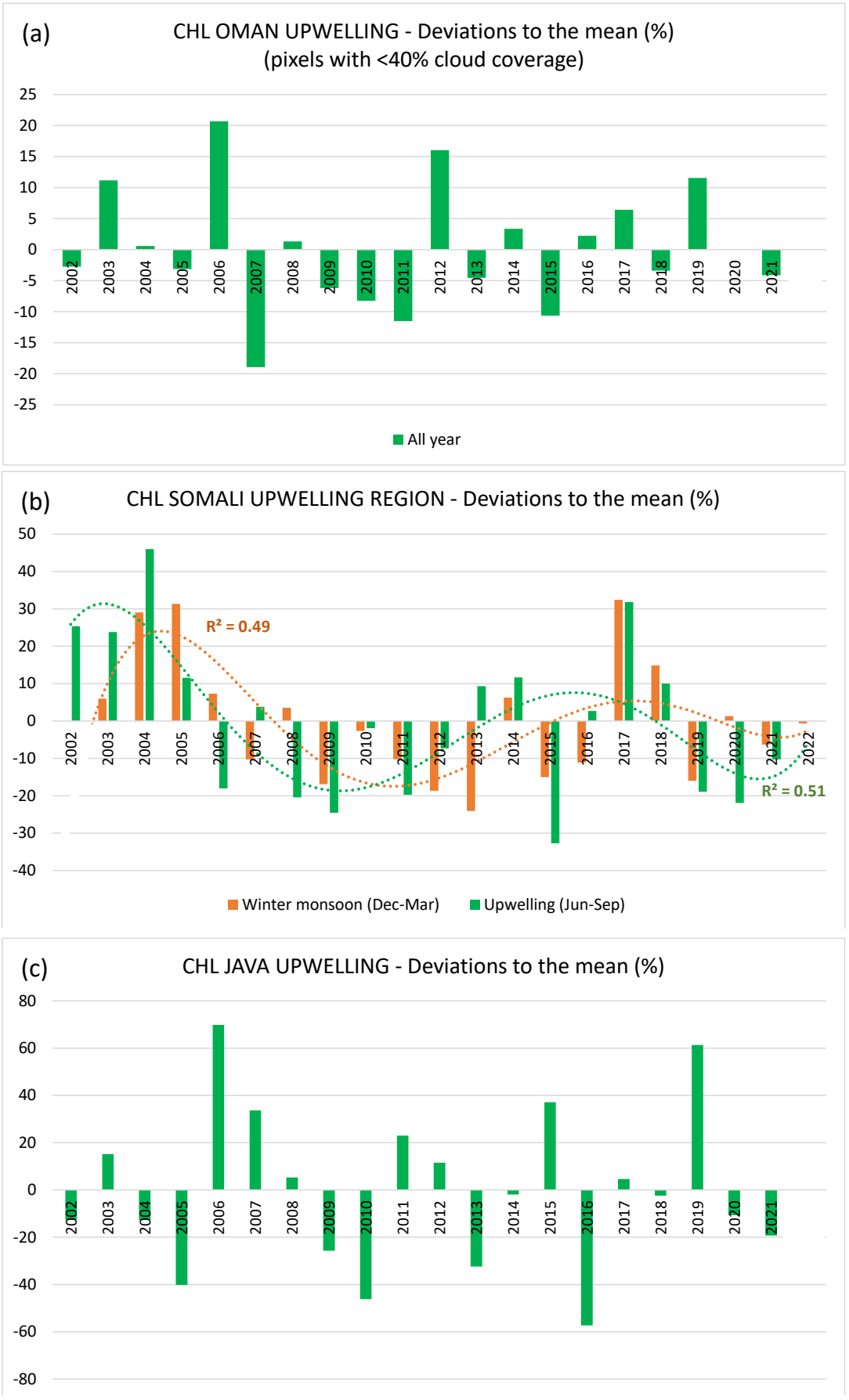

Fig. 12 – Chlorophyll concentration (standardized as deviation in % to the mean) in three upwelling systems of the Indian Ocean, for 2002-2022.